

Self-organized shocks in the sedimentation of a granular gas

Lidia Almazán,¹ Dan Serero,¹ Clara Salueña,² and Thorsten Pöschel¹¹*Institute for Multiscale Simulation, Universität Erlangen-Nürnberg, D-91052 Erlangen, Germany*²*Departament d'Enginyeria Mecànica, Universitat Rovira i Virgili, 43007 Tarragona, Spain*

(Received 15 February 2014; published 26 June 2015)

A granular gas in gravity heated from below develops a certain stationary density profile. When the heating is switched off, the granular gas collapses. We investigate the process of sedimentation using computational hydrodynamics, based on the Jenkins-Richman theory, and find that the process is significantly more complex than generally acknowledged. In particular, during its evolution, the system passes several stages which reveal distinct spatial regions of inertial (supersonic) and diffusive (subsonic) dynamics. During the supersonic stages, characterized by $\text{Mach} > 1$, the system develops supersonic shocks which are followed by a steep front of the hydrodynamic fields of temperature and density, traveling upward.

DOI: [10.1103/PhysRevE.91.062214](https://doi.org/10.1103/PhysRevE.91.062214)

PACS number(s): 45.70.Mg

I. INTRODUCTION

Granular gases, that is, ensembles of macroscopic particles with internal degrees of freedom interacting by binary collisions, are intensively studied since they reveal a rather exotic behavior as compared to molecular gases, originating from the dissipative nature of particle collisions (see [1], and many references therein). In particular, the dynamics of granular gases as well as more dense granular systems is frequently characterized by supersonic behavior. While the supersonic nature of rapid granular flows is known for long time (see, e.g., [2], and references therein), it was shown that supersonic behavior may appear also in force-free systems as a result of self-organized dynamics [3]. Later, Tan and Goldhirsch [4] showed that supersonic behavior is not an exotic state but dynamical granular systems are nearly always supersonic, that is, it is a *typical* state of granular matter. There is much recent progress regarding the supersonic properties of granular matter, including shocks, theoretically [5–9], numerically [10–17], and experimentally [7–9, 18–24]; however, surprisingly little is known about the spatiotemporal relation between the field of Mach number influenced by temperature and density and the dynamics of supersonic shocks in granular systems [25–27].

While since the pioneering study by McNamara and Young [28] the collapse of a free granular gas undoubtedly pertains to the most extensively studied nonstationary granular phenomena, the important issue of collapse occurring under external forcing has, on the other hand, seldom been addressed. A simple experimentally feasible example of such a process consists in the sedimentation of a granular gas under the action of gravity. To persist under conditions of gravity, granular gases need the external support of energy to balance the loss of energy due to dissipative collisions. While in experiments energy is frequently supplied via vibration of the confinement or parts of it, theoretical approaches often consider a *heated wall*, i.e., a solid boundary reemitting incoming particles with a velocity sampled from a distribution corresponding to the temperature of the wall. A granular gas under gravity heated from below exhibits a nonmonotonous stationary density profile [29,30], in contrast to the barometric profile in molecular gases. The corresponding temperature profile decays with height, due to dissipative collisions.

Starting from this stationary state, in this paper we investigate the evolution of the system when we switch off the supply of energy and the granular gas sediments under the action of gravity.

Such a process was first considered by Volfson *et al.* [31] who found by numerical integration of hydrodynamic equations and particle simulations that the energy of the gas drops to zero in finite time, $E \sim (t_c - t)^2$. This behavior is surprising as it resembles a single particle in gravity: Starting at velocity v_0 , the velocity after the k th impact is $\varepsilon^k v_0$ where ε is the coefficient of restitution. The k th impact takes place at time

$$t_k = \sum_{n=0}^{k-1} \frac{2v_0}{g} \varepsilon^n = \frac{2v_0}{g} \frac{1 - \varepsilon^k}{1 - \varepsilon} = \frac{2v_0}{g(1 - \varepsilon)} \left(1 - \frac{v_k}{v_0}\right). \quad (1)$$

Solving for v_k and dropping the index we obtain

$$v = \frac{g}{2}(1 - \varepsilon)(t_c - t) \quad \text{with} \quad t_c \equiv \frac{2v_0}{g(1 - \varepsilon)}. \quad (2)$$

Therefore, energy decays like $E \sim (t_c - t)^2$, which is the same functional form as found for the granular gas. From this result it may be concluded that the sedimentation of the granular gas is the same way as independently moving particles, that is, the interaction of particles seems to be unimportant for the functional form of the decay of energy.

Later in [32], Son *et al.* investigated the same problem experimentally, leaving a previously vibrated granular gas to condense under the action of gravity. They confirmed $E \approx (t_c - t)^\beta$; however, $\beta = 3.1 \dots 6.1$ was found. Son *et al.* measured the hydrodynamic fields of density, temperature, and vertical velocity and identified two distinct stages in the process of sedimentation, separated by a steep increase of temperature which they call a settling shock. In order to explain the differences between the energy decay laws found from hydrodynamic theory [31] and in experiments [32], Kachuck and Voth [33] performed particle simulations for a wide parameter range to reproduce the results of [32].

Using numerical hydrodynamics analysis, in the present paper we show that the process of sedimentation is more complex than generally acknowledged. In particular, the sedimentation process comprises several stages, where only the last one is the (diffusive) scaling regime with the critical time, t_c , identified in [31,32]. This behavior is preceded by

a sequence of shock front scenarios whose spatiotemporal appearance is attributed to the field of Mach number and its relation to the fields of density and temperature. While the term “shock” was used also in [31,32] to characterize a steep gradient of the fields of density or temperature, here we show that the term shock applies in its genuine meaning, that is, as a boundary between diffusive and inertial dynamics characterized by the appearance of supersonic flow. Surprisingly, the spatial and temporal appearance of these true shocks does not agree with the effects termed shock in [31,32].

II. HYDRODYNAMIC DESCRIPTION

Consider a granular gas of smooth inelastic hard disks of mass m and diameter σ colliding with a constant coefficient of restitution ε . The hydrodynamic fields of number density, $n(\vec{r}, t)$, flow velocity, $\vec{u}(\vec{r}, t)$, and temperature, $T(\vec{r}, t)$, obey the balance equations [34]

$$\begin{aligned} \frac{\partial n}{\partial t} + \vec{\nabla} \cdot (n\vec{u}) &= 0, \\ \rho \left(\frac{\partial \vec{u}}{\partial t} + \vec{u} \cdot \vec{\nabla} \vec{u} \right) &= -\vec{\nabla} \cdot \hat{P} + \rho \vec{g}, \\ n \left(\frac{\partial T}{\partial t} + \vec{u} \cdot \vec{\nabla} T \right) &= -\nabla \cdot \vec{q} - \hat{P} : \vec{\nabla} \vec{u} - \zeta n T, \end{aligned} \quad (3)$$

where $\rho = mn$, \vec{g} , \hat{P} , \vec{q} , and ζ denote mass density, gravity, pressure, heat flux, and cooling rate due to dissipative collisions, respectively. The constitutive relations for pressure and heat flux are

$$\begin{aligned} P_{ij} &= p\delta_{ij} - \eta(\partial_j u_i + \partial_i u_j - \delta_{ij} \vec{\nabla} \cdot \vec{u}) - \gamma\delta_{ij} \vec{\nabla} \cdot \vec{u}, \\ \vec{q} &= -\kappa \vec{\nabla} T \end{aligned} \quad (4)$$

with p , η , γ , and κ standing for hydrostatic pressure, shear and bulk viscosity, and thermal conductivity. Their explicit forms are provided by the Jenkins-Richman theory [34]:

$$\begin{aligned} p &= \frac{4}{\pi\sigma^2} \phi T [1 + (1 + \varepsilon)G(\phi)], \\ \eta &= \frac{\phi}{2\sigma} \sqrt{\frac{mT}{\pi}} \left[\frac{1}{G(\phi)} + 2 + \left(1 + \frac{8}{\pi}\right)G(\phi) \right], \\ \kappa &= \frac{2\phi}{\sigma} \sqrt{\frac{T}{\pi m}} \left[\frac{1}{G(\phi)} + 3 + \left(\frac{9}{4} + \frac{4}{\pi}\right)G(\phi) \right], \\ \gamma &= \frac{8}{\pi\sigma} \phi G(\phi) \sqrt{\frac{mT}{\pi}}, \quad \zeta = \frac{4}{\sigma} (1 - \varepsilon^2) \sqrt{\frac{T}{\pi m}} G(\phi), \end{aligned} \quad (5)$$

where $\phi = n\pi\sigma^2/4$ is the packing fraction, $G(\phi) = \phi\chi(\phi)$, and $\chi(\phi)$ is the pair correlation function [35] with the random close packing fraction for disks, $\phi_{\max} = 0.82$.

During the sedimentation, the system shows simultaneously regions of low and high density, therefore, the solution of the compressible Navier-Stokes equations, Eq. (3), is a numerical challenge requiring a highly precise but numerically expensive weighted essentially nonoscillatory (WENO) scheme [36–38] which was shown to deliver reliable results for rather similar systems [26]. During the sedimentation, with progressing time the top region of the system would reach zero density while the sediment at the bottom approaches dense packing. Numerical

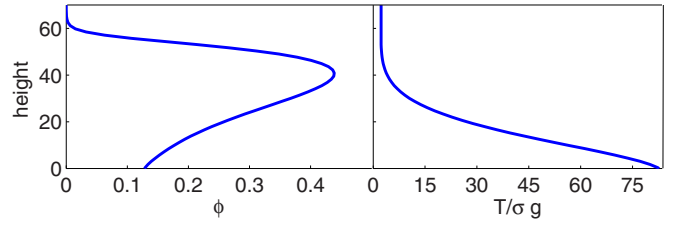


FIG. 1. (Color online) Stationary profiles of packing fraction, $\phi(y)$, and temperature, $T(y)$, of a granular system heated from below, $T_0 = 10^6$, establishing the initial conditions of the sedimentation. Height is given in units of σ .

hydrodynamics codes cannot handle these limits, therefore our code restricts density to $0.0001 \leq \phi \leq 0.9999\phi_{\max}$ while preserving the total mass.

For later use, we define the (local) speed of sound,

$$c_s^2 = \frac{\partial p}{\partial n} + \frac{p}{n^2} \frac{\partial p}{\partial T}, \quad (6)$$

for the (local) hydrostatic pressure, p [see Eq. (5)].

When the system is supplied with energy from below through a thermal wall at temperature T_0 , it adopts a stationary state with characteristic profiles of packing fraction and temperature [30] which is the initial state of the sedimentation process starting at time $t = 0$ when the heating is switched off. From this moment on we assume adiabatic boundary conditions (zero heat flux) at the bottom. At the top, density vanishes due to gravity, implying zero heat flux as well. Consequently the loss of energy in the course of time is exclusively due to inelasticity of the particle collisions. The amount of granular material was chosen such that the height of the sediment at $t \rightarrow \infty$ is 20 layers of particles. Figure 1 shows the initial state for the system specified by box size $L_x = 50\sigma$ (periodic boundary conditions) and $L_y = 300\sigma$, coefficient of restitution $\varepsilon = 0.98$, total mass equivalent $N = 1044$ particles at random close packing, ϕ_{\max} , and $T_0 = 10^6$.

III. DECAY OF ENERGY

Let us first look to the evolution of the total energy, Fig. 2, revealing a complex behavior which may be attributed to different stages of the gas discussed in detail below.

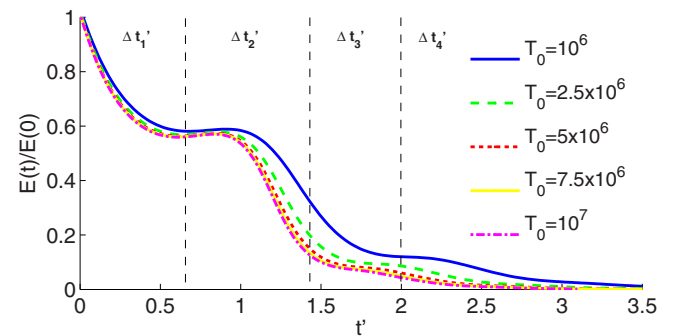


FIG. 2. (Color online) Total energy as a function of time for different values of the initial bottom plate temperature, T_0 . Dashed lines indicate the stages of the sedimentation process.

Remarkably, in scaled time, $t' \equiv t/\sqrt{T_0/g^2}$, with increasing T_0 the curves approach a generic line, that is, for $T_0 \gtrsim 10^7$ they virtually collapse [39]. This scaling allows us to describe the process of sedimentation independently of the value of T_0 .

IV. STAGES OF THE SEDIMENTATION PROCESS

We simulate the process using the parameters specified above. It was checked that the results do not qualitatively differ for other choices, except for the coefficient of restitution which will be discussed below. Figure 3 shows the evolution of the fields of density, velocity, temperature, and Mach $\equiv |\vec{v}|/c_s$, after switching off the supply of energy. Starting from the initial condition, Fig. 1, after a very short transient during which the particles accelerate in gravity, the gas immediately expands [Fig. 3(a)], somewhat counterintuitively (see below). During the first stage of its evolution, $\Delta t'_1$, the material is hot and loose, dissipating the energy contained in the lower part of the system, and actually increasing in density everywhere except for a small expanding region which corresponds to the area where the first shock wave emerges at $\Delta t'_2$. The latter manifests itself through the formation of a supersonic region accompanied by a density front moving downward (Fig. 4), corresponding to the fall of the material having expanded above the transition region. Indeed, in the second stage, $\Delta t'_2$, the material deposits in the lower part while the upper part is cold enough to become supersonic and shock waves may emerge. Here and in the subsequent figures, red symbols indicate the vertical position where Mach = 1: For larger height, the regime is inertial; here supersonic shock waves propagate while for smaller height, diffusion dominates. For times when no symbol is drawn, the regime is diffusive everywhere. Thus, in $\Delta t'_2$, a loose and supersonic granular layer collides at the bottom where the deposit starts to form. The energy of the collision is partly propagated upward in the form of a shock wave associated with an abrupt increase of temperature [Fig. 3(c)], causing expansion of the upper

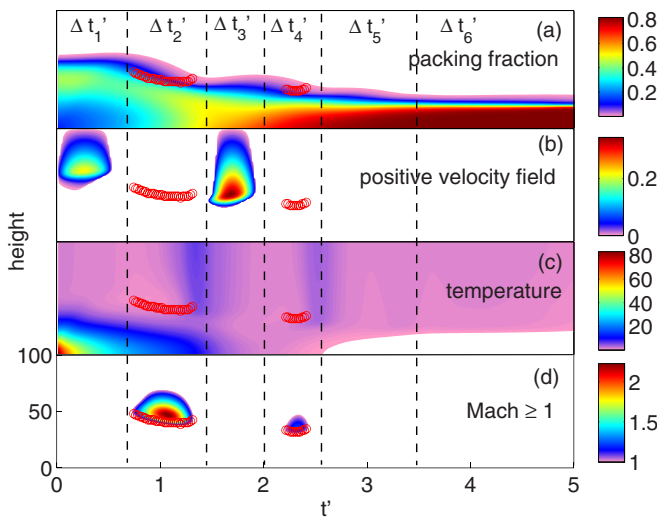


FIG. 3. (Color online) Evolution of the hydrodynamic fields. Red circles indicate the vertical location where Mach=1. Scale of the vertical axis is the same for all graphs (here given only for Mach). Height is given in units of σ .

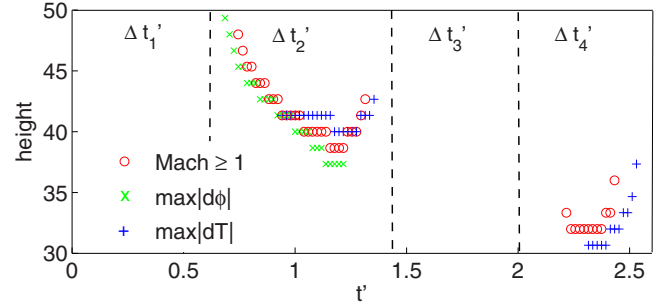


FIG. 4. (Color online) Location of the maximal slope of the temperature and density profiles, as a function of time. Circles indicate Mach=1. Height is given in units of σ .

part which takes place in $\Delta t'_3$. Subsequently, in $\Delta t'_4$ we see a second sedimentation phase involving previously expanded material in coexistence with a condensed phase below 20σ in height. Again, the material accelerates downward due to gravity, and eventually becomes supersonic. In this stage, the sediment at the bottom is already immobilized, that is, its energy has virtually disappeared. Consequently, the energy of the emerging shock leads only to a very weak expansion and sedimentation cycle following in $\Delta t'_5$, much less pronounced as it involves much less material close to the surface. The energy of the material is almost entirely dissipated by the sediment such that no further expansion-sedimentation cycles can emerge. By varying the parameters of the simulations, except ε , we could not observe more than two intervals of supersonic behavior (see below). Finally, $\Delta t'_6$ is the stage of residual deposition: the bottom layer is already compacted and motion throughout the system is scarce; here the transport mechanism is essentially diffusive. This is the domain of the scaling regime reported in [31], where the material is almost at rest, such that thermal conduction is the dominant heat transfer mechanism, that is, the regime is clearly subsonic.

The described scenario corresponds to the experimental results reported in [32]. Indeed, if we compare the distinct regions sketched in Fig. 3 we distinguish essentially the same areas as in [32], except that the second inertial regime cannot be appreciated in the experiments since the first rebound is already weak due to the dissipative sediment.

Figure 3(b) which depicts the areas having positive macroscopic velocities, indicates that during $\Delta t'_1$, the system is separated into two parts moving in opposite directions, the lowest part settling downward, increasing the density at the bottom plate, while the upper region of the gas moves upward. This is due to the fact that in the transition area, the pressure increases faster than in the rest of the system: This area indeed corresponds to the maximal density of the initial condition (Fig. 1), rendering the pressure more sensitive to density changes. Similarly, during the second expansion phase $\Delta t'_3$, the material is separated between an upper part moving upward and a lower moving downward (the transition region being again the area where the shock forms during $\Delta t'_4$), but the latter is actually very small: This part corresponds to almost settled sediment; therefore, while for $\Delta t'_2$ the particles collide with the adiabatic bottom, for $\Delta t'_3$ the particles collide with a very dissipative sediment dissipating all incoming energy rapidly. In other words, at time between $\Delta t'_2$ and $\Delta t'_3$ the floor

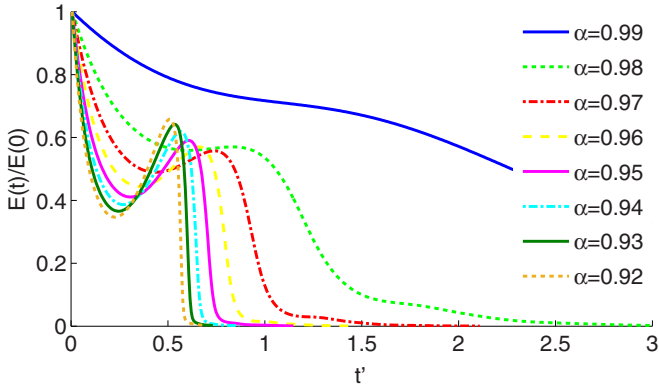


FIG. 5. (Color online) Decay of the total energy for different coefficient of restitution ($T_0 = 10^7$).

of the system changes quickly from adiabatic (zero heat flux) to conducting (large heat flux), which in turn suppresses further rebound.

Figure 3(d) indicates that the region of $\text{Mach} \geq 1$ spreads over a large part of the system during the first inertial period. In contrast, during the second inertial period, $\text{Mach} \geq 1$ only for a small vertical interval such that the shock wave can travel only a small vertical distance.

The correlation between the steep slopes of the hydrodynamic fields and the transition between subsonic and supersonic regions can be clearly seen in Fig. 4, where the locations of the transition are plotted together with the maxima of the gradients of density and temperature. Both shock fronts are accompanied by jumps in the hydrodynamic fields.

V. COEFFICIENT OF RESTITUTION

The scenario in scaled time, t' , is essentially independent of the system parameters, except for the coefficient of restitution which was chosen $\varepsilon = 0.98$ so far. In experiments, Son

et al. [32] used glass spheres with $\varepsilon = 0.98$ and $\varepsilon = 0.92$ for interparticle collisions and particle and plate collisions, respectively, finally considering $\varepsilon = 0.95$ for the whole system in their comparison with theory. Therefore, we performed simulations for the same interval (Fig. 5). While we identify similar stages for all ε considered, the curves appear stretched for small inelasticity. Moreover, for $\varepsilon \lesssim 0.95$, the second plateau disappears. Consequently, for $\varepsilon \lesssim 0.95$, we see only one shock wave pulse, similar to the experiments by Son *et al.* [32].

VI. CONCLUSIONS

We investigated the sedimentation of a granular cloud using computational hydrodynamics, based on the Jenkins-Richman theory, and find that the process is significantly more complex than generally acknowledged. In particular, during its evolution, the system passes several stages which reveal distinct spatial regions of inertial (supersonic) and diffusive (subsonic) dynamics. In scaled time, the evolution is independent of initial conditions for large enough temperature of the bottom plate. During the supersonic stages, characterized by $\text{Mach} > 1$, the system develops supersonic shocks which are followed by sharp profiles of the hydrodynamic fields of temperature and density. Whereas these sharp profiles have been reported in the literature before based on theoretical and experimental work, the appearance of supersonic shocks was not mentioned before. Also in agreement with earlier findings, for more dissipative material ($\varepsilon \lesssim 0.95$) the shock dynamics consists of a single phase.

ACKNOWLEDGMENTS

We thank the Kompetenznetzwerk für wissenschaftliches Höchstleistungsrechnen in Bayern (KONWIHR) for funding. The German Science Foundation (DFG) is acknowledged for funding through its Cluster of Excellence “Engineering of Advanced Materials.”

-
- [1] I. Goldhirsch, *Annu. Rev. Fluid Mech.* **35**, 267 (2003).
 - [2] A. Goldshtein, M. Shapiro, and C. Gutfinger, *J. Fluid Mech.* **316**, 29 (1996).
 - [3] S. E. Esipov and T. Pöschel, *J. Stat. Phys.* **86**, 1385 (1997).
 - [4] M. L. Tan and I. Goldhirsch, *Phys. Rev. Lett.* **81**, 3022 (1998).
 - [5] I. Goldhirsch, *Chaos* **9**, 659 (1999).
 - [6] B. Meerson, I. Fouxon, and A. Vilenkin, *Phys. Rev. E* **77**, 021307 (2008).
 - [7] J. F. Boudet, J. Cassagne, and H. Kellay, *Phys. Rev. Lett.* **103**, 224501 (2009).
 - [8] J. F. Boudet and H. Kellay, *Phys. Rev. E* **87**, 052202 (2013).
 - [9] S. P. Pudasaini and C. Kroner, *Phys. Rev. E* **78**, 041308 (2008).
 - [10] V. Buchholtz and T. Pöschel, *Granular Matter* **1**, 33 (1998).
 - [11] P. Zamankhan, *Shock Waves* **17**, 337 (2008).
 - [12] P. Zamankhan, *Phys. Fluids* **21**, 043301 (2009).
 - [13] L. Almazan, J. A. Carrillo, C. Salueña, V. Garzo, and T. Pöschel, *New J. Phys.* **15**, 043044 (2013).
 - [14] S. N. Pathak, Z. Jabeen, P. Ray, and R. Rajesh, *Phys. Rev. E* **85**, 061301 (2012).
 - [15] R. Yano and K. Suzuki, *Eur. Phys. J. E* **34**, 31 (2011).
 - [16] A. Soleymani, P. Zamankhan, and W. Polashenski, *Appl. Phys. Lett.* **84**, 4409 (2004).
 - [17] C. R. Wassgren, J. A. Cordova, R. Zenit, and A. Karion, *Phys. Fluids* **15**, 3318 (2003).
 - [18] E. C. Rericha, C. Bizon, M. D. Shattuck, and H. L. Swinney, *Phys. Rev. Lett.* **88**, 014302 (2001).
 - [19] J. Bougie and K. Duckert, *Phys. Rev. E* **83**, 011303 (2011).
 - [20] J. F. Boudet, Y. Amarouchene, and H. Kellay, *Phys. Rev. Lett.* **101**, 254503 (2008).
 - [21] Y. Amarouchene and H. Kellay, *Phys. Fluids* **18**, 031707 (2006).
 - [22] J. F. Boudet and H. Kellay, *Phys. Rev. Lett.* **105**, 104501 (2010).
 - [23] G. Hu, Y. Li, M. Hou, and K. To, *Phys. Rev. E* **81**, 011305 (2010).

- [24] K. Huang, G. Q. Miao, P. Zhang, Y. Yun, and R. J. Wei, *Phys. Rev. E* **73**, 041302 (2006).
- [25] J. Bougie, Sung Joon Moon, J. B. Swift, and H. L. Swinney, *Phys. Rev. E* **66**, 051301 (2002).
- [26] J. A. Carrillo, T. Pöschel, and C. Salueña, *J. Fluid Mech.* **597**, 119 (2008).
- [27] K. Huang, P. Zhang, G. Miao, and R. Wei, *Ultrasonics* **44**, e1487 (2006).
- [28] S. McNamara and W. R. Young, *Phys. Fluids A* **4**, 496 (1992).
- [29] J. J. Brey and M. J. Ruiz-Montero, *Phys. Rev. E* **67**, 021307 (2003).
- [30] B. Meerson, T. Pöschel, and Y. Bromberg, *Phys. Rev. Lett.* **91**, 024301 (2003).
- [31] D. Volfson, B. Meerson, and L. S. Tsimring, *Phys. Rev. E* **73**, 061305 (2006).
- [32] R. Son, J. A. Perez, and G. A. Voth, *Phys. Rev. E* **78**, 041302 (2008).
- [33] S. B. Kachuck and G. A. Voth, *Phys. Rev. E* **88**, 062202 (2013).
- [34] J. T. Jenkins and M. W. Richman, *Phys. Fluids* **28**, 3485 (1985).
- [35] S. Torquato, *Phys. Rev. E* **51**, 3170 (1995).
- [36] G. Jiang and C.-W. Shu, *J. Comput. Phys.* **126**, 202 (1996).
- [37] C.-W. Shu, in *Advanced Numerical Approximation of Nonlinear Hyperbolic Equations*, edited by A. Quarteroni, Lecture Notes in Mathematics Vol. 1697 (Springer, Berlin, 1998), pp. 325–432.
- [38] More precisely, the compressible Navier-Stokes equations [Eq. (3)] are solved by a fifth-order finite-difference characteristicwise WENO method for the Euler terms on a uniform grid, second-order central finite differences for source terms. The resulting ordinary differential equation system is solved in time by an explicit third-order total variation diminishing (TVD) Runge-Kutta scheme. WENO yields high order accuracy in smooth regions and essentially nonoscillatory transitions near strong discontinuities [36,37]. For details on the numerical scheme, see [26].
- [39] The scaling of time can be obtained from a detailed analysis of Eqs. (3)–(5) which shall be published elsewhere.